Vibrationally resolved O 1s photoelectron spectrum of water

R. Sankari [a], M. Ehara [b], H. Nakatsuji [b], Y. Senba [c], K. Hosokawa [c],
H. Yoshida [c], A. De Fanis [d], Y. Tamenori [d], S. Aksela [a], K. Ueda [e,*]

[a] *Department of Physical Sciences, P.O. Box 3000, 90014 University of Oulu, Finland*
[b] *Department of Synthetic Chemistry and Biological Chemistry, Graduate School of Engineering,*
Kyoto University, Sakyou-ku, Kyoto 606-8501, Japan
[c] *Department of Physical Science, Hiroshima University, Higashi-Hiroshima 739-8526, Japan*
[d] *SPring-8/JASRI, Sayou-gun, Hyogo 679-5198, Japan*
[e] *Institute of Multidisciplinary Research for Advanced Materials, Tohoku University, Sendai 980-8577, Japan*

Abstract

The O 1s photoelectron spectrum of water was recorded with the resolution high enough to resolve the vibrational structure of the O $1s^{-1}$ state and the lifetime width and the Franck-Condon (FC) factors were extracted. The experimental spectrum was reproduced well by the molecular ab initio calculations based on the symmetry adapted cluster-configuration interaction (SAC-CI) method. The vibrational structure was attributed mostly to the bending mode of the core-ionized molecule.
© 2003 Elsevier B.V. All rights reserved.

1. Introduction

Recently, water has been under extensive studies, not only because of its fundamental biological role but also by its importance in astrophysics. Although the absorption, ion yield and resonant Auger spectra are under active study (see, e.g. [1–4], and references therein), the measurement of the O 1s photoelectron spectrum of water dates back to 1960s [5]. At that time, however, the experimental resolution using the conventional X-ray source was not sufficient to resolve the vibrational

structure of the core-ionized molecule. The Auger decay following the O 1s ionization of water was also studied earlier both experimentally [6] and theoretically [7].

The O 1s photoionization of water and its decay of O $1s^{-1}$ state were studied theoretically by Cesar et al. [8]. The ab initio calculations provide valuable information about the lifetime and the vibrational energy spacing of the core-ionized state. At the time of the study [8], however, there was no experimental photoelectron spectrum with sufficient resolution to compare with the theoretical results. Furthermore, computers as well as computational methods have improved significantly in the last decades. Therefore, it is interesting to re-investigate theoretically the photoelectron spectrum and

---

* Corresponding author. Fax: +81-22-217-5405.
E-mail address: ueda@tagen.tohoku.ac.jp (K. Ueda).

compare the results with previous theoretical ones, as well as with the new experimental results.

The ground state water molecule belongs to C_{2v} point group and its electronic configuration is

$$1a_1^2 \; 2a_1^2 \; 1b_2^2 \; 3a_1^2 \; 1b_1^2 \; (^1A_1),$$

where $1a_1$ and $2a_1$ are almost pure O 1s and 2s orbitals, respectively, whereas the remaining three orbitals have more hybrid-orbital character. As a C_{2v} nonlinear molecule consisting of three atoms, the water molecule has three vibrational modes; the symmetric stretching and bending modes of a_1 symmetry and the antisymmetric stretching mode of b_2 symmetry. In the first approximation, the only vibrational modes of a_1 symmetry are expected to be excited when the 1s core level of the central O atom is ionized.

In the present work, the O 1s photoelectron spectrum of water is recorded with high experimental resolution. The core-ionized $1a_1^{-1}$ state is investigated also theoretically by means of the SAC/SAC-CI method [9–11]. The SAC/SAC-CI method has been successfully applied to various molecular spectroscopies including ionization processes. In the series of applications, the SAC-CI general-R method [12,13] has clarified the fine details of the main and satellite spectra (e.g. [14,15]) in the outer- and inner-valence regions. In the present work, we demonstrate that this method is powerful also to simulate the core-level photoelectron spectra.

2. Experimental

The measurements were carried out at the c branch of the beam line 27SU at SPring-8, a synchrotron radiation facility with an 8-GeV storage ring in Japan. The figure-8 undulator installed in this beam line produces high-intensity linearly polarized soft X-rays. When integer order (i.e., 1st, 2nd, etc.) harmonics of the undulator radiation are chosen, the light is horizontally polarized whereas the half-integer (i.e., 0.5th, 1.5th, etc.) harmonics provide vertically polarized light [16]. The radiation is guided to a Hettrick type monochromator that covers the photon energy range of 150–2500 eV with three different gratings. A more detailed description of the beam line and the monochromator can be found elsewhere [17,18]. The photon energy scale was calibrated using the CO_2 excitation energies reported by Prince et al. [19].

The ejected electrons were analyzed with an SES-2002 electron energy analyzer equipped with a gas cell: both were manufactured by Gammadata Scienta Ab. The binding energy scale was calibrated by measuring the O 1s spectrum of O_2, whose binding energy values were measured by Sorensen et al. [20] with an accuracy of ± 0.02 eV. The transmission function of the electron energy analyzer was supposed to be a constant in such a short kinetic energy region: retardation ratio varied between 0.39 and 0.41. The analyzer broadening corresponding to 500 μm entrance slit and 20 eV pass energy is about 40 meV (FWHM). The photoelectron spectrum was recorded at 590 eV photon energy with the photon bandwidth of approximately 50 meV. The overall experimental broadening, including Doppler broadening [21], was thus estimated to be about 70 meV.

For precise determination of the lifetime width of the core-ionized state of water, the photoelectron spectrum of Xe 5p was measured using the same experimental settings as with water. The line-profile of the Xe 5p photoelectron line, well described by the 70 meV wide Gaussian line-shape, was expected to represent also the instrumental broadening of the O 1s photoelectron spectrum of water after replacing the Doppler broadening of Xe with corresponding value of water.

3. Theoretical

The three-dimensional (3D) potential energy surfaces (PESs) of the ground and $1a_1^{-1}$ core-ionized states were calculated and the vibrational spectrum was simulated from them. The flexible basis set was used to describe the orbital reorganization and the electron correlations of the inner-shell ionized state; TZV [5s3p/3s] of Ahlrichs' group [22] augmented with two polarization d-functions ($\zeta_d = 1.615, 0.6375$) for O and one p-function ($\zeta_p = 1.0$) for H. The core-ionized state was calculated by the SAC-CI method. In the SAC-CI, a core–valence separation approximation

was adopted and the *R*-operators were restricted to those including the core–hole molecular orbital (MO). The SAC-CI wavefunction for the inner-shell ionized state is given by

$$\Psi_{\text{SAC-CI}} = \left(R_{\text{I}} + \sum_{ja} R_{\text{I}j}^{a} + \sum_{jkab} R_{\text{I}jk}^{ab} \right) \exp(S) |\Psi_{\text{HF}}\rangle,$$

(1)

where j, k and a, b are occupied and unoccupied MOs, respectively, I denotes the $1a_1$ orbital [12,13]. For $|\Psi_{\text{HF}}\rangle$, the ground-state Hartree–Fock with the canonical MOs was used. From the preliminary examinations, the effect of this approximation was found to be small and the *R*-operators were included up to triples. All the MOs were included in the active space for describing the core–hole relaxation. In order to reduce the computational effort, the operators were selected within the state-selection scheme [23]. For the ground state, all the single and double linked terms were included and the unlinked terms were selected as the products of the important linked terms whose single–double excitation configuration–interaction coefficients were larger than 0.005. For the ionized state, all the single and double operators were included and the energy threshold of triples was set to $\lambda_e = 1.0 \times 10^{-6}$. The thresholds of the CI coefficients for calculating the unlinked operators in the SAC-CI method were 0.01 and 0.0 for the *R* and *S* operators, respectively.

For calculating the vibrational spectrum, 3D vibrational states were obtained by the grid method, in which Lanczos algorithm was adopted for the diagonalization. In the present study, 3D PESs were described in the binding coordinates, where the OH distances are r_1 and r_2, and θ defines the angle between the two axes. In these coordinates the kinetic part of the Hamiltonian ($J = 0$) of the vibrational motion is given by

$$T = \frac{p_1^2}{2\mu_{\text{OH}}} + \frac{p_2^2}{2\mu_{\text{OH}}} + \frac{j^2}{2\mu_{\text{OH}}r_1^2} + \frac{j^2}{2\mu_{\text{OH}}r_2^2}$$
$$+ \frac{p_1 p_2 \cos\theta}{m_{\text{O}}} - \frac{p_1 p_\theta}{m_{\text{O}} r_2} - \frac{p_2 p_\theta}{m_{\text{O}} r_1}$$
$$- \frac{\cos\theta j^2 + j^2 \cos\theta}{2m_{\text{O}} r_1 r_2},$$

(2)

where

$$p_k = -\mathrm{i}\frac{\partial}{\partial r_k} \quad (k = 1, 2), \qquad p_\theta = -\mathrm{i}\frac{\partial}{\partial \theta}\sin\theta,$$

$$j^2 = -\frac{1}{\sin\theta}\frac{\partial}{\partial\theta}\sin\theta\frac{\partial}{\partial\theta},$$

(3)

and μ_{OH} is the reduced mass of O and H atoms [24]. The coordinates r_1 and r_2 are represented by the sine discrete variable representation (DVR) with 30 points and θ is by the Legendre DVR of 50 points. The 3D PESs of the ground and $1a_1^{-1}$ states were calculated at 567 different structures in the region of $0.8 \leqslant r_1, r_2 \leqslant 1.2$ Å and $90° \leqslant \theta \leqslant 150°$, and were fitted by the fifth-order Morse-cosine expansion

$$V(r_1, r_2, \theta) = \sum_{i,j,k=0}^{5} [B_{ijk}(1 - \mathrm{e}^{-a(r_1-r_e)})^i$$
$$\times (1 - \mathrm{e}^{-a(r_2-r_e)})^j (\cos\theta - \cos\theta_e)^k],$$

(4)

where r_e and θ_e were equilibrium values of each state and were determined by the analytical energy gradients of the SAC/SAC-CI method [25,26].

Finally, the vibrational spectrum of the $1a_1^{-1}$ state was simulated using the 3D PESs determined by the SAC/SAC-CI method. The 3D vibrational wavefunctions and the FC factors were obtained by diagonalizing the vibrational Hamiltonian ($J = 0$) given by Eqs. (2) and (4). Note that in the previous MCSCF work [8] the spectrum was calculated using the 2D harmonic approximation.

The SAC/SAC-CI calculations were executed using the SAC-CI96 program system [27], which has been incorporated into the development version of the GAUSSIAN suite of programs [28]. For calculating the vibrational states and the FC factors, MCTDH program package [29] was used.

4. Results and discussion

The equilibrium structures for the potential energy surfaces of the ground and $1a_1^{-1}$ states of water, harmonic frequencies of these states and the adiabatic ionization potential (IP) with the zero-point energy correction are summarized in Table 1

Table 1
Experimental and theoretical equilibrium geometry and spectroscopic constants of the ground and $1a_1^{-1}$ states of H_2O

	Experimental [31]	This work		MC-SCF [8]	ΔSCF [30]
		Experimental	SAC-CI		
X^1A_1					
R_e (Å)	0.9578	–	0.9581	0.9635	0.9435
θ_e (°)	104.48	–	105.17	105.3	106.7
ω_1 (meV)	475	–	467	479	516
ω_2 (meV)	204	–	210	209	217
ω_3 (meV)	489	–	484	–	528
$^2A_1$ ($1a_1^{-1}$)					
R_e (Å)	–	–	0.9652	0.967	0.9472
θ_e (°)	–	–	118.62	119	122.4
ω_1 (meV)	–	460(20)	438	448	492
ω_2 (meV)	–	159(5)	177	166	176
ω_3 (meV)	–	–	442	–	508
IP	–	539.79(2)	539.55	539.58	539.42

IPs of the present theoretical work and ΔSCF are with the zero-point energy correction, whereas IP of MC-SCF is without the zero-point energy correction.

together with the experimental values and other earlier theoretical results [8,30]. The equilibrium structure of the ground state is calculated to be $r_e = 0.9581$ Å and $\theta_e = 105.17°$ which are in very good agreement with the experimental values of $r_e = 0.9584$ Å and $\theta_e = 104.48°$ [31]. The geometry relaxation in the $1a_1^{-1}$ ionized state is insignificant for r, $\Delta r = 0.007$ Å, but remarkably large for θ, $\Delta\theta = 13.45°$. This causes the vibrational progression of the bending mode in the O 1s photoelectron spectrum. This trend agrees with the previous MCSCF [8] and ΔSCF [30] calculations. Fig. 1 displays the potential energy curves of the ground and $1a_1^{-1}$ states of water as a function of the angles in the range $90° \leqslant \theta \leqslant 150°$, with respect to the cut of the 3D surfaces for constant r at the equilibrium length r_e. In the figure, one can clearly see the displacement of the potential minimum of the $1a_1^{-1}$ state from that of the ground and state. It is also clear from Fig. 1 that the 3D PESs calculated by the SAC-CI method, within the region of interest, are suitable for calculating the vibrational levels and the Franck–Condon (FC) factors. The harmonic frequencies of the ground state are calculated to be 467, 210, and 484 meV, for the symmetric stretching (ω_1), bending (ω_2) and antisymmetric stretching (ω_3), respectively. All the harmonic frequencies of the $1a_1^{-1}$ state are esti-
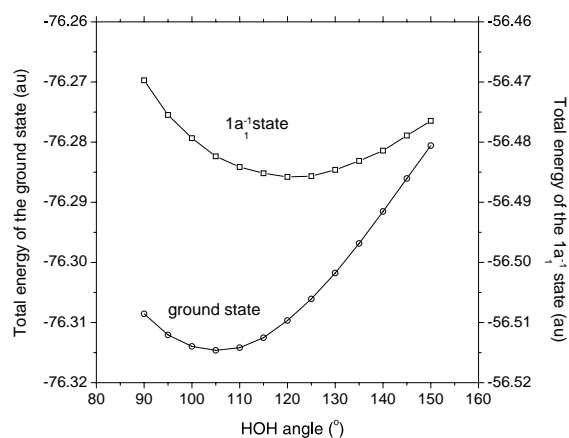

Fig. 1. The potential energy curves of the ground and $1a_1^{-1}$ states of water as a function of the angles in the range $90° \leqslant \theta \leqslant 150°$, with respect to the cut of the 3D surfaces for constant r at the equilibrium length r_e, calculated by the SAC/SAC-CI method.

mated smaller by approximately 30–40 meV in comparison with those of the ground state, as shown in Table 1. The adiabatic and vertical IPs are calculated to be 539.60 and 539.67 eV, respectively. The IP, taking account the zero-point energy correction, is evaluated to be 539.55 eV.

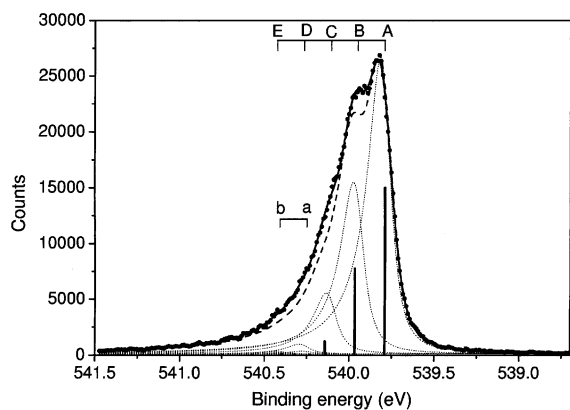In Fig. 2, the SAC-CI spectrum of the $1a_1^{-1}$ state is compared with the experimental spectrum. The

Fig. 2. Photoelectron spectrum of oxygen 1s of water excited at 590 eV photon energy. Full circles show the experimental data taken at 0° relative to polarization vector of incident radiation whereas the thick solid line gives the final least-squares fit for the whole spectrum. Dotted lines represent the individual fitted vibrational lines before the convolution with the instrumental function. Dashed line presents the theoretical spectrum (shifted up by 0.24 eV in binding energy); the theoretical Franck–Condon factors are given by the vertical lines (see text for details). The labels A–E refer to the components of the first fitted progression whereas a and b refer to the second one.

O 1s ionized state of water decays mainly by non-radiative Auger electron emission. Therefore, the photoelectron spectrum was fitted using the post-collision interaction (PCI) distorted line-shapes. The theoretical components presented as columns in Fig. 2 were also convoluted to produce the same line-profile as in the experimental spectrum: the resulting spectrum is presented by a dashed line in Fig. 2. The line-profile is a convolution of intrinsic line-shape with the instrumental function modeled by the Gaussian shape. The width of the instrumental function is obtained from the Xe 5p measurement as described earlier. The intrinsic asymmetric line-shape is described by the PCI line-profile given by Armen et al. [32]. The PCI profile is determined by the natural lifetime width, the photoelectron energy and the Auger electron energy. The kinetic energy of the Auger electrons is estimated from the early measurement of Siegbahn et al. [6], taking the weighted average based on the spectrum in [6]. The lifetime width and the photoelectron energy are treated as fitting parameters. The energy shift between the actual resonance energy (i.e., photoelectron energy of each vibrational component) and the energy position of the peak maximum in Fig. 2 is also due to the PCI effect. All the fitted results are obtained using the least-squares fitting procedure [33] which allows linking of the fitting parameters.

Two progressions with the same vibrational frequency, taken as a free parameter in the fitting procedure, were fitted into the experimental spectrum. The binding energy, the lifetime width and the vibrational spacing of the core-ionized state were extracted from the fitting results. The experimental values obtained are presented in Table 2 together with present theoretical values. According to the theoretical vibrational frequencies, the strongest vibrational progression (labeled with capital letters A–E) can be assigned to the $(0, n, 0)$ bending vibrations. The experimental vibrational frequency, 159 ± 5 meV is, however, slightly smaller than the corresponding theoretical value (see Table 2). The second, much weaker progression

Table 2
Experimental and theoretical excitation energies and Franck–Condon factors of O $1s^{-1}$ state in water

Label	Assignment	ΔE_{theory}	$\Delta E_{\text{exper.}}$	$\text{FCF}_{\text{theory}}$	$\text{FCF}_{\text{exper.}}$
A	$(0, 0, 0)$	0.000	0.000	1.000	1.000
B	$(0, 1, 0)$	0.177	0.159	0.519	0.571(3)
C	$(0, 2, 0)$	0.354	0.318	0.083	0.190(3)
a	$(1, 0, 0)$	0.438	0.460	0.004	0.004(7)
	$(0, 0, 1)$	0.442	–	0.000	–
D	$(0, 3, 0)$	0.529	0.477	0.006	0.033(7)
b	$(1, 1, 0)$	0.610	0.619	0.008	0.010(5)
	$(0, 1, 1)$	0.616	–	0.000	–
E	$(0, 4, 0)$	0.703	0.636	0.000	0.006(4)
	$(1, 2, 0)$	0.785	–	0.004	–

All the excitation energies are given relative to $1s^{-1}(0, 0, 0)$ state. Labels refer to Fig. 2.

with only two components (labeled as a and b) could be assigned to the $(1, n, 0)$ symmetric stretching vibration by comparing to the calculated values. There are some $(0, n, 1)$ antisymmetric vibrations in the same region but they were omitted in the fitting because of the symmetry reasons, which were confirmed by the present theoretical results. Although the second progression could be fitted to the experimental spectrum, the values should be considered cautiously as the uncertainties for such weak underlying structures are in general large. The agreement with theoretical values is reasonable: the FC factors of the strongest vibrational structures are reproduced well. However, there are some discrepancies between the theoretical and the experimental FC factors: the present calculations underestimate slightly all the FC factors relative to $(0, 0, 0)$ component and the discrepancy increases with an increase in the vibrational quantum number n. This tendency can be clearly seen by comparing the experimental and theoretical FC factors of both progressions and by the difference between the experimental and theoretical spectra of Fig. 2. The origin of this discrepancy may stem from the fact that the ω_2, i.e., the curvature at the potential minimum of the $1a_1^{-1}$ state in Fig. 1, is slightly overestimated in the calculation.

The experimentally determined ionization energy of O $1s^{-1}$ state, 539.79 ± 0.02 eV, is in reasonable agreement with the value (539.82 eV) extrapolated from the high resolution total ion yield measurement of Okada et al. [34]. The present theoretical ionization energy, 539.55 eV, is in reasonable agreement with the experimental value. The lifetime width of the O $1s^{-1}$ core–hole state, as extracted from the fitting, is 160 ± 5 meV, which is slightly bigger than the theoretical value of 150 meV presented by Carravetta and Ågren [35]. The angular distribution parameter β was extracted from the fitting results. The value $\beta = 1.8(1)$ was found the same for all fitted components within statistical uncertainties; the results are not unexpected as the measurement was done quite far from the ionization threshold.

In conclusion, the natural line-width of the O $1s^{-1}$ state of water was determined from the high-resolution photoelectron spectrum. The vibrational structures, i.e., the vibrational spacings and FC factors, related to the core–hole ionized state of water, were partly resolved; the large natural width of the O $1s^{-1}$ state of water hinders more detailed analysis. The calculated spectroscopic constants agreed well with the corresponding experimental values. The vibrational structures were attributed mainly to the $(0, n, 0)$ bending mode; the symmetric stretching vibrations have some contribution to the higher binding energy region of the spectrum.

Acknowledgements

References

[1] M.N. Piancastelli, A. Hempelmann, F. Heiser, O. Gessner, A. Rüdel, U. Becker, Phys. Rev. A 59 (1999) 300.

[2] A. Hiraya, K. Nobusada, M. Simon, K. Okada, T. Tokushima, Y. Senba, H. Yoshida, K. Kaminori, H. Okumura, Y. Shimizu, A.-L. Thomas, P. Millie, I. Koyano, K. Ueda, Phys. Rev. A 63 (2001) 042705.

[3] I. Hjelte, M.N. Piancastelli, R.F. Fink, O. Björneholm, M. Bässler, R. Feifel, A. Giertz, H. Wang, K. Wiesner, A. Ausmees, C. Miron, S.L. Sorensen, S. Svensson, Chem. Phys. Lett. 334 (2001) 151.

[4] A. De Fanis, K. Nobusada, I. Hjelte, N. Saito, M. Kitajima, M. Okamoto, H. Tanaka, H. Yoshida, A. Hiraya, I. Koyano, M.N. Piancastelli, K. Ueda, J. Phys. B 35 (2002) L23.

[5] K. Siegbahn, C. Nordling, G. Johansson, J. Hedman, P.F. Hedèn, K. Hamrin, U. Gelius, T. Bergmark, L.O. Werme, R. Manne, Y. Baer, ESCA Applied to Free Molecules, North-Holland, Amsterdam, 1969.

[6] H. Siegbahn, L. Asplund, P. Kelfve, Chem. Phys. Lett. 35 (1975) 330.

[7] H. Ågren, O. Vahtras, J. Phys. B 26 (1993) 913.

[8] A. Cesar, H. Ågren, V. Carravetta, Phys. Rev. A 40 (1989) 187.

[9] H. Nakatsuji, Chem. Phys. Lett. 59 (1978) 362.

[10] H. Nakatsuji, Chem. Phys. Lett. 67 (1979) 329.

[11] H. Nakatsuji, in: Computational Chemistry – Review of Current Trends, vol. 2, World Scientific, Singapore, 1997, p. 62.

[12] H. Nakatsuji, J. Chem. Phys. 83 (1985) 713, 5743; H. Nakatsuji, J. Chem. Phys. 94 (1991) 6716.

[13] H. Nakatsuji, Chem. Phys. Lett. 177 (1991) 331.

[14] M. Ehara, H. Nakatsuji, Chem. Phys. Lett. 282 (1998) 347.

[15] M. Ehara, M. Ishida, K. Toyota, H. Nakatsuji, in: K.D. Sen (Ed.), Reviews in Modern Quantum Chemistry, World Scientific, Singapore, 2002.

[16] T. Tanaka, H. Kitamura, J. Synchrotron Radiation 3 (1996) 47.

[17] H. Ohashi, E. Ishiguro, Y. Tamenori, H. Kishimoto, M. Tanaka, M. Irie, T. Ishikawa, Nucl. Instr. Meth. A 467 (2001) 529.

[18] H. Ohashi, E. Ishiguro, Y. Tamenori, H. Okumura, A. Hiraya, H. Yoshida, Y. Senba, K. Okada, N. Saito, I.H. Suzuki, K. Ueda, T. Ibuki, S. Nagaoka, I. Koyano, T. Ishikawa, Nucl. Instr. Meth. A 467 (2001) 533.

[19] K.C. Prince, L. Avaldi, M. Coreno, R. Camilloni, M. de Simone, J. Phys. B 32 (1999) 2551.

[20] S.L. Sörensen et al., to be published.

[21] P. Baltzer, L. Karlsson, M. Lundqvist, B. Wannberg, Rev. Sci. Instrum. 64 (1993) 2179.

[22] A. Schaefer, C. Huber, R. Ahlrichs, J. Chem. Phys. 100 (1994) 5829.

[23] H. Nakatsuji, Chem. Phys. 75 (1983) 425.

[24] M.H. Beck, H.-D. Meyer, J. Chem. Phys. 114 (2001) 2036.

[25] T. Nakajima, H. Nakatsuji, Chem. Phys. Lett. 280 (1997) 79; T. Nakajima, H. Nakatsuji, Chem. Phys. 242 (1999) 177.

[26] M. Ishida, K. Toyota, M. Ehara, H. Nakatsuji, Chem. Phys. Lett. 347 (2001) 493.

[27] H. Nakatsuji, M. Hada, M. Ehara, J. Hasegawa, T. Nakajima, H. Nakai, O. Kitao and K. Toyota, SAC/SAC-CI program system (SAC-CI96) for calculating ground, excited, ionized, and electron-attached states having singlet to septet spin multiplicities, 1996.

[28] M.J. Frisch et al., GAUSSIAN 99, Revision A.8, Gaussian Inc., Pittsburgh, PA, 1998.

[29] G.A. Worth, M.H. Beck, A. Jäckle, H.-D. Meyer, The MCTDH Package, Version 8.3, University Heidelberg, Heidelberg, Germany, 2003.

[30] J.A. Smith, P. Jørgensen, Y. Öhrn, J. Chem. Phys. 62 (1975) 1285.

[31] A.R. Hoy, I.M. Mills, G. Strey, Mol. Phys. 24 (1972) 1265.

[32] G.B. Armen, J. Tulkki, T. Åberg, B. Crasemann, Phys. Rev. A 36 (1987) 5606.

[33] H.M. Köppe, A.L.D. Kilcoyne, J. Feldhaus, A.M. Bradshaw, J. Electron Spectrosc. Relat. Phenom. 75 (1995) 97.

[34] K. Okada, K. Ueda, T. Tokushima, Y. Senba, H. Yoshida, Y. Shimizu, M. Simon, H. Chiba, H. Okumoru, Y. Tamenori, H. Ohashi, N. Saito, S. Nagaoka, I.H. Suzuki, E. Ishiguro, I. Koyano, T. Ibuki, A. Hiraya, Chem. Phys. Lett. 326 (2000) 314.

[35] V. Carravetta, H. Ågren, Phys. Rev. A 35 (1987) 1022.